Experimental Investigation of Vortex Breakdown over a Delta Wing with Consideration of Control by Fluid Injection

P. Molton[*], A. Mitchell[**], D. Barberis[*], D. Afchain[*], O. Rodriguez[*], J. Pruvost[*]
[*]ONERA/DAFE
8 rue des Vertugadins
92190 Meudon, France

[**]U.S. Air Force Academy
2354 Fairchild Drive, Suite 6H27
Colorado Springs CO 80840-6222, USA

Abstract

This paper gives the results of two experiments on control of vortex breakdown on a delta wing by fluid injection. The first was conducted in a wind tunnel on a wing with a 70-degree sweep. It focused on characterizing vortex breakdown through analysis of the unsteady pressures on the wing's suction surface, with the aim of defining a detection mode as a control input for feedback control. Control by along-the-core fluid injection, near the apex, caused downstream movement of vortex breakdown that was detected by field measurements and surface pressure sensors.

The second experiment, in a water tunnel, concerned a wing with a 60-degree sweep. Fluid was injected at different locations along the wing's upper surface. The results demonstrated the effectiveness of injecting momentum to control vortex breakdown.

1 Introduction

Much experimental and theoretical research has been conducted on the flow structure existing on the upper surface of a delta wing [1, 2, 3, 4, 5, 6], because of its applications related to combat aircraft flying at high angles of attack.

It is well-known that at high angles of attack, multiple vortex structures form on the wing due to the rolling-up of the viscous shear layers which separate from the upper surface. The highest energy structures result from separation along the so-called primary separation line, which is the leading edge, if it is sharp or highly curved. The intensity of this main vortex increases with the angle of attack until a sudden disorganization occurs. This phenomenon, known as vortex breakdown, is characterized by rapid deceleration of both the axial and the tangential mean velocity components inside the vortex. During breakdown, the axial mean velocity component vanishes then becomes negative on the axis of the vortex, corresponding to appearance in the flow structure of a stagnation point followed by a recirculation bubble. Large-scale fluctuations arise at the same time.

At ONERA, work on vortex breakdown [7, 8] first focused on investigating the breakdown of an isolated vortex in order to characterize the main influence parameters: form of velocity distributions, and intensity of the external pressure gradient [9]. During the second stage, the aerodynamic field above the wing, more complex due to the interaction between vortex breakdown and the pressure field induced by the wing in the presence of breakdown, was investigated [10].

This paper discusses the effects of injecting fluid to control vortex breakdown. It contains data from two different experimental studies. For greater clarity, the results are presented separately, since they correspond to tests conducted under different experimental conditions. In the first case, the tests were conducted in a wind tunnel on a delta wing with a 70-degree sweep, placed in a subsonic flow. The focus was to identifying the vortex breakdown location by measuring unsteady surface pressures with the aim of defining a breakdown indicator for a feedback control system. The second experiment, conducted in a water tunnel, concerned a delta wing with a 60-degree sweep. Here, the emphasis was on interpretation of the flow field visualizations and the breakdown phenomenology. The effects of control by fluid injection were measured using a force balance.

Paper presented at the RTO AVT Symposium on "Advanced Flow Management: Part A – Vortex Flows and High Angle of Attack for Military Vehicles", held in Loen, Norway, 7-11 May 2001, and published in RTO-MP-069(I).

Report Documentation Page

Form Approved
OMB No. 0704-0188

1. REPORT DATE	2. REPORT TYPE	3. DATES COVERED
00 MAR 2003	**N/A**	**-**

4. TITLE AND SUBTITLE	5a. CONTRACT NUMBER
Experimental Investigation of Vortex Breakdown Over a Delta Wing With Consideration of control by Fluid Injection	5b. GRANT NUMBER
	5c. PROGRAM ELEMENT NUMBER
6. AUTHOR(S)	5d. PROJECT NUMBER
	5e. TASK NUMBER
	5f. WORK UNIT NUMBER
7. PERFORMING ORGANIZATION NAME(S) AND ADDRESS(ES) **NATO Research and Technology Organisation BP 25, 7 Rue Ancelle, F-92201 Neuilly-Sue-Seine Cedex, France**	8. PERFORMING ORGANIZATION REPORT NUMBER
9. SPONSORING/MONITORING AGENCY NAME(S) AND ADDRESS(ES)	10. SPONSOR/MONITOR'S ACRONYM(S)
	11. SPONSOR/MONITOR'S REPORT NUMBER(S)

12. DISTRIBUTION/AVAILABILITY STATEMENT
Approved for public release, distribution unlimited

13. SUPPLEMENTARY NOTES
Also see: ADM001490, Presented at RTO Applied Vehicle Technology Panel (AVT) Symposium held inLeon, Norway on 7-11 May 2001, The original document contains color images.

14. ABSTRACT

15. SUBJECT TERMS

16. SECURITY CLASSIFICATION OF:			17. LIMITATION OF ABSTRACT	18. NUMBER OF PAGES	19a. NAME OF RESPONSIBLE PERSON
a. REPORT	b. ABSTRACT	c. THIS PAGE			
unclassified	**unclassified**	**unclassified**	**UU**	**14**	

2 Wind Tunnel Investigation of Vortex Breakdown on a Delta Wing with a 70-Degree Sweep

2.1 Experimental Set-up and Test Conditions

The tests were conducted in ONERA's Fauga-Mauzac F2 wind tunnel, a closed-return atmospheric wind tunnel whose test section, 5 m long, has a rectangular cross section 1.4 m wide and 1.8 m high. The maximum wind speed in the tunnel is 100 m/s. The model used was a delta wing with a 70-degree sweep and a 950 mm chord, made of a 20 mm thick flat plate with a leading edge having a 15-degree bevel on the lower surface.

The model was equipped with 17 Kulite^{TM} unsteady pressure sensors distributed along the span ($0.5 \le Y/e \le 0.7$, where e is the local half-span) at X = 500, 600, 700 and 800 mm. The injection devices were located near the wing apex at 14 percent of the chord and in the axes of the vortex cores. The compressed air jet was thus transported to the vortex core by the transverse velocity component. Each device included a tapered movable nozzle with an outlet diameter of 2.07 mm. Downstream, the U-shaped exit channel cut into the thickness of the wing had an inclination of 15.6 degrees and a length of 26 mm. Figure 1 is a diagram of the injection device.

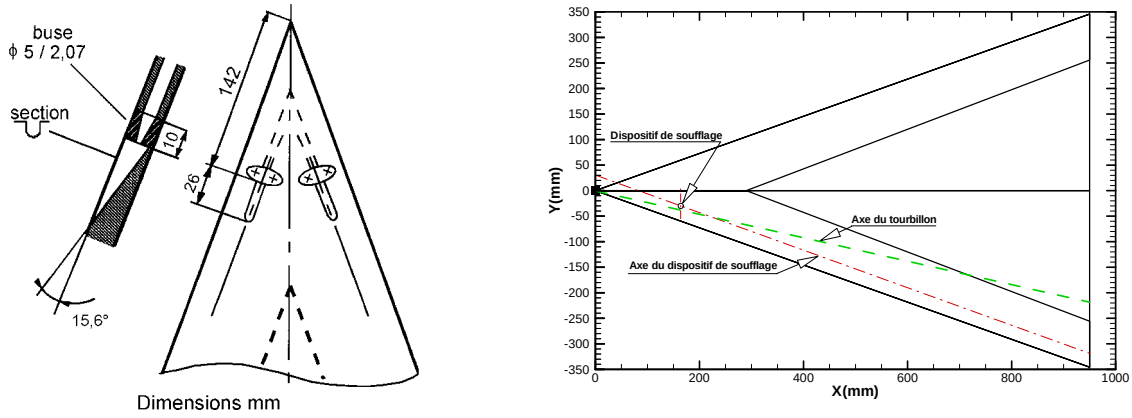

Fig. 1 – Definition of the injection device

Injection was produced by solenoid valves that output a continuous or pulsed compressed air jet. The solenoid valves are individually controlled from a PC. In pulsed mode, they were opened and closed in phase or out of phase. The results are given as injection mass flow rate Q_m and momentum flow coefficient:

$$C_\mu = \frac{Q_m V_j}{1/2 \rho U_0^2 S}$$

where V_j is the air jet velocity, ρ is the density, U_0 is the uniform upstream velocity and S is the wing surface area.

The tests were conducted at a freestream velocity of U_0 = 24 m/s corresponding to a chord based Reynolds number of 1.56×10^6.

2.2 Presentation of the Results

Mean vortex breakdown location. Figure 2 shows the results obtained by laser sheet visualization techniques for an angle of attack α = 26 degrees, in which can be seen development of the primary vortex on the wing. The vortex axis is shown as a black line between its origin at the apex and the breakdown point, located approximately 650 mm from the apex for this angle of attack. It is characteristic of a vortex rotating at a fast rate. The particles seeding the flow are ejected from the core of the structure by centrifugal forces. Vortex breakdown is accompanied by expansion of the vortex core and a decrease in the centrifugal forces applied to the tracer particles, which can then penetrate

close to the center of the vortex, allowing its visualization. In addition, the strong flow fluctuations promote seeding of the entire structure.

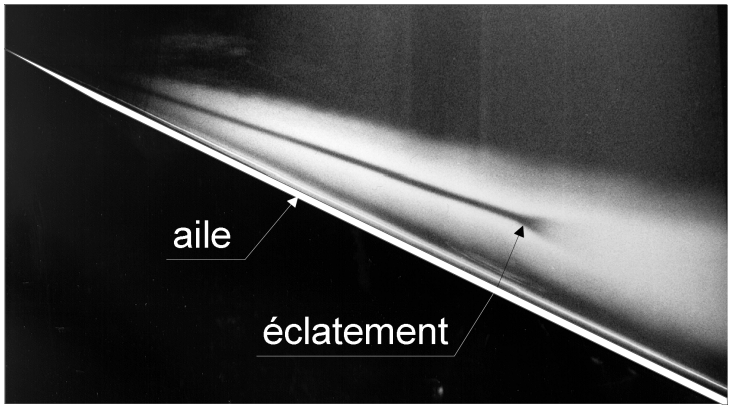

Fig. 2 - Vortex breakdown by laser sheet visualization. α = 26 degrees, U_0 = 24 m/s

Figure 3 shows the variation of vortex breakdown location versus angle of attack α. For a given value of α, a line represents all the breakdown locations determined from several pictures. The dispersion of the points reflects the amplitude of the breakdown location fluctuations.

It can be seen that the mean value of vortex breakdown location moves upstream as the angle of attack increases. Breakdown occurs on the trailing edge for an angle of attack α = 25 degrees. Small variations of the breakdown location are observed for α = 26 degrees and α = 27 degrees, whereas the streamwise location varies substantially for angles of attack between 28 degrees and 32 degrees. Above α = 32 degrees, the breakdown location again stabilizes.

The dispersion of the results reflects the unsteady nature of the phenomenon [11]. The width of the envelope of extreme breakdown locations is at a maximum for an angle of attack $\alpha \approx 30$ degrees where the breakdown is located at mid-chord.

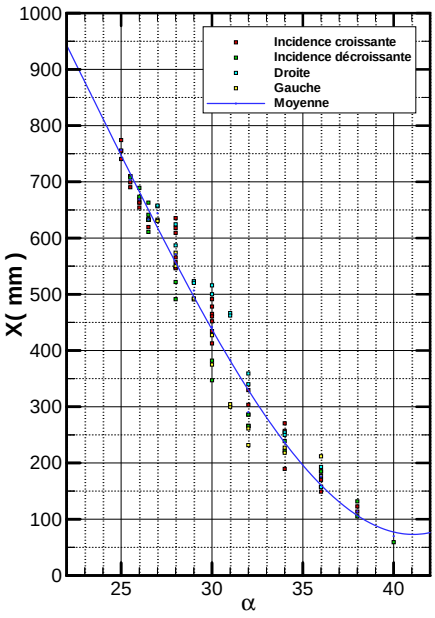

Fig. 3 – Variation of breakdown location versus angle of attack

Breakdown detection by measurement of the unsteady surface pressure. Laser sheet visualization shows development of the breakdown region resulting in the dissipation of the rapidly rotating central vortex region and its replacement by a recirculation region. For the mean surface pressure measurements, these phenomena result in attenuation of the low pressure minimum related to the vortex. However, the surface pressure distributions do not allow detection of vortex breakdown until the recirculation region has developed enough to exert a significant trace on the surface of the model.

Unsteady pressure measurements were realized to determine a characteristic frequency (or frequency range) of the oscillating breakdown location, thus allowing more accurate detection of the breakdown effect on the surface by suitably analyzing the output signals. Figure 4 shows the variations in power spectral density for sensors located below the vortex axis in four different abscissas and for different model angles of attack ($20° \leq \alpha \leq 32°$). These curves demonstrate detection of vortex breakdown through an increase in power spectral density and the appearance of a frequency peak between 40 and 110 Hz, corresponding to a Strouhal number $S = fc/U_0$ between 1.58 and 3.96.

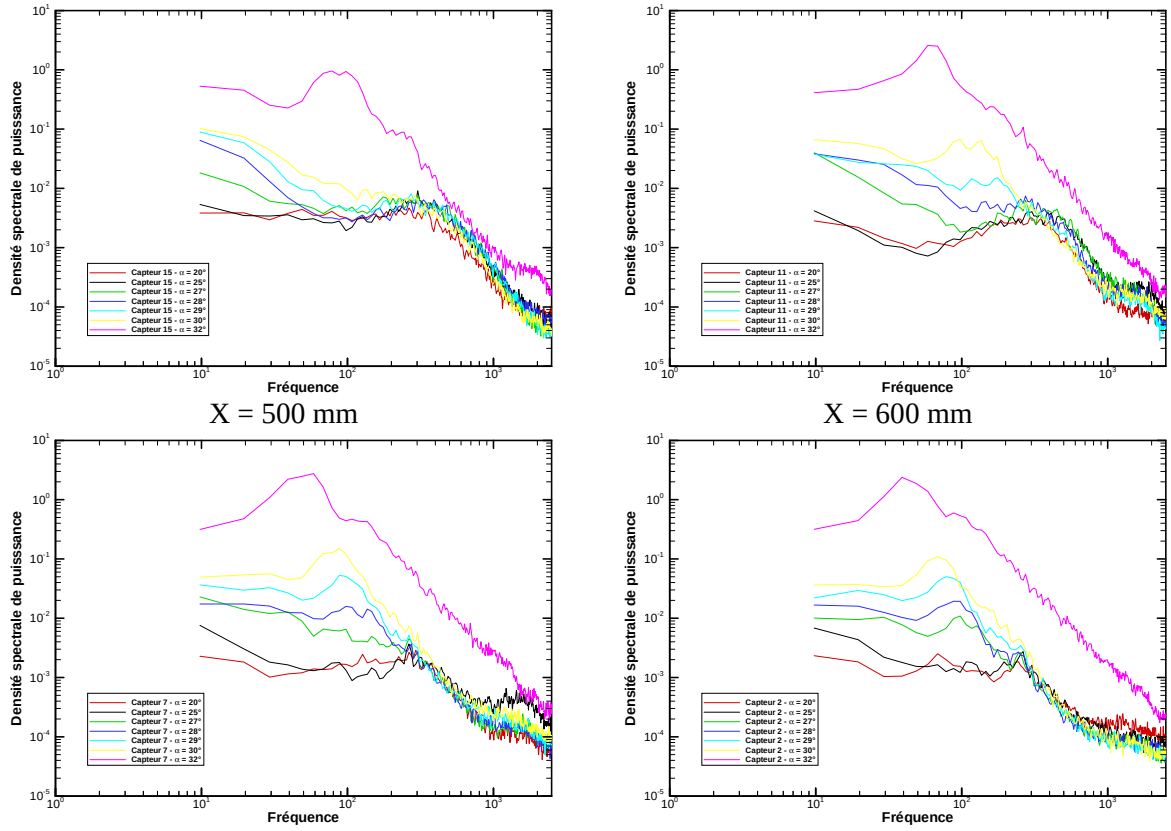

X = 500 mm X = 600 mm

X = 700 mm X = 800 mm

Fig. 4 – Variation of power spectral density versus frequency. Nominal configuration.

Considering the results for the sensor at X = 500 mm, it can be seen that the frequency peak is observable only for α = 32 degrees. For this configuration, Figure 3 shows vortex breakdown is located at X = 330 mm. The frequency peak characteristic of vortex breakdown is observable in the unsteady surface pressure distributions 170 mm downstream of the average vortex breakdown location. However, due to the scarcity of sensors along the vortex axis, it was not possible to accurately determine the minimum vortex breakdown detection distance. No characteristic frequency peaks are observed in the results for α = 29 degrees and α = 30 degrees. For these two configurations, vortex breakdown occurs at X = 495 mm for α = 29 degrees and X= 430 mm for α = 30 degrees, corresponding to distances from the sensor of 5 and 70 mm respectively.

Figure 4b shows the results for the section at X = 600 mm. A power spectral density peak is observed for angles of attack α = 29 degrees, 30 degrees and 32 degrees. The breakdown locations are X_e = 495 mm, X_e = 430 mm and X_e = 330 mm respectively for these configurations. The results show that vortex breakdown is detectable for a distance of 105 mm for α = 29 degrees and 170 mm for α = 30 degrees. The configuration at α = 28 degrees, giving a vortex breakdown location of X_e = 570 mm, does not exhibit a power spectral density peak. However, from X = 700 mm on (see Fig. 4c), the sensor used at this abscissa exhibits a spectral density peak starting at α = 28 degrees.

In addition, it should be noted that this power spectral density extremum is obtained at an increasingly low frequency as the distance between the vortex breakdown location and the unsteady

pressure sensor increases. This evaluation is confirmed by the results obtained with the sensor located at X = 800 mm. In this section, development of an extremum is observed for α = 27 degrees. For this configuration, vortex breakdown was located at X_e = 617 mm. It was not evidenced in the section at X = 700 mm, corresponding to a distance of 83 mm from the breakdown location. Finally, it should be noted that the results at α = 25 degrees do not exhibit a characteristic peak for this configuration. The distance between the vortex breakdown location and the sensor was then 60 mm.

The unsteady pressure sensors are able to detect vortex breakdown from the instantaneous surface pressure distributions. However, detection is possible only at or above a distance of around 100 mm downstream of the vortex breakdown location as identified by laser sheet visualization techniques. The above results show that the frequency decreases when the distance between the pressure sensor and the influence of the breakdown on the surface increase. The frequency ranges between 40 and 110 Hz. Figure 5 shows the different frequencies where power spectral density extremum were observed versus the distance between the vortex breakdown locations measured by laser sheet visualization techniques, and the abscissa at which the unsteady pressure sensor was located. Despite the dispersion in the results, primarily due to the small number of sensors, the correlation between the frequency corresponding to an extremum and the distance to the breakdown location is good.

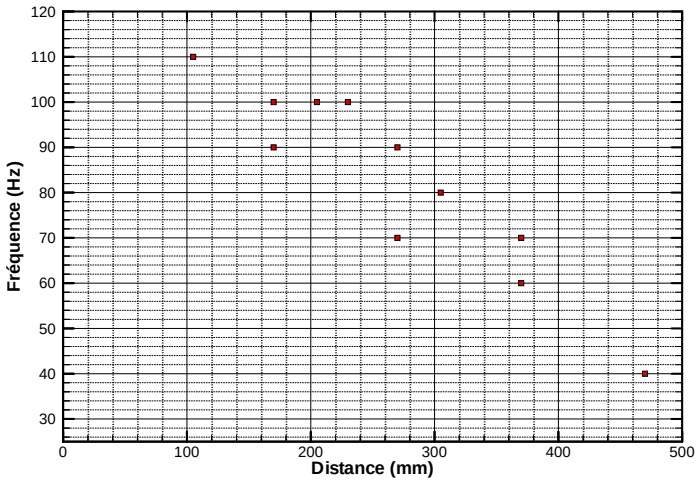

Fig. 5 – Frequency variation versus influence distance

Additionally, it can be seen that for the configurations where vortex breakdown occurs on the leeward side of the wing, an increase in the angle of attack corresponds to an increase in the extremum of the power spectral density.

Effect of control by continuous injection. During this study, six cases of control by injection were investigated: three continuous injection configurations and three pulsed injection configurations. This study is summarized in the table below.

Injection rate	1.8 g/s	2.2 g/s	3.2 g/s
Continuous			
Pulsed			0.5 Hz 1 Hz 10 Hz

Summary of injection conditions

A longitudinal plane through the vortex axis was explored by laser doppler velocimetry between X = 300 mm and X = 600 mm, at increments ΔX of 25mm, corresponding to a mesh with 292 points. In the case of control by injection, the plane was explored between X = 300 mm and X = 675 mm, at increments ΔX of 25mm, corresponding to a mesh with 388 points. Figure 6 shows the iso-distributions of the axial velocity component (U/U_0) for the nominal configuration and a configuration with control by injection with a mass flow rate Q_m = 2.2 g/s, i.e. C_μ = 0.006. It can be seen that the velocity increases along the vortex axis, then suddenly decreases, leading to the appearance of a stagnation point in the flow with development of a recirculation region and an increase in the vortex core diameter.

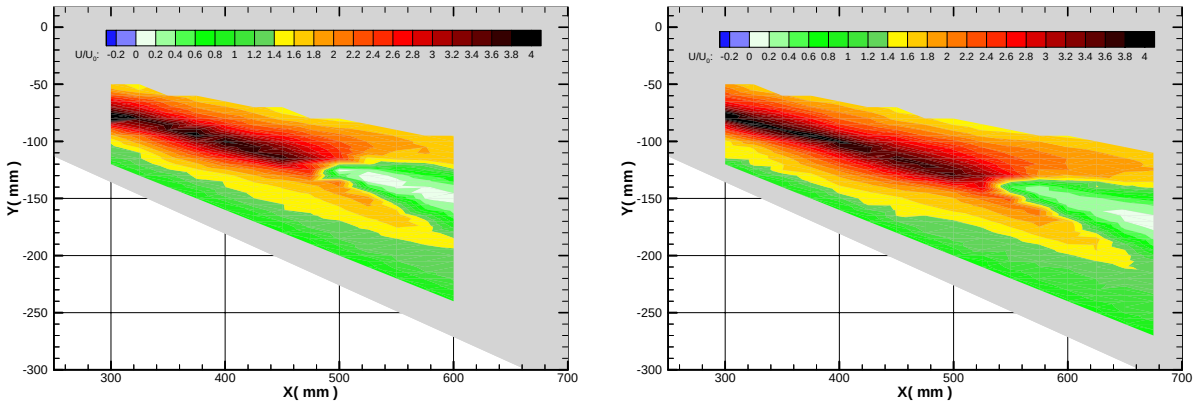

a - Nominal configuration

b - Control by continuous injection at Q_m = 2.2 g/s (C_μ = 0.006)

Fig. 6 – Constant axial velocity component distributions. a) Nominal configuration. b) Control by continuous injection at Q_m = 2.2 g/s (C_μ = 0.006). Angle of attack α = 30 degrees

In Figure 6a (nominal configuration), the vortex breakdown location is situated at X ≈ 475 mm (X/c ≈ 0.5). In Figure 6b (continuous injection at Q_m = 2.2 g/s, C_μ = 0.006), the estimated location of the vortex breakdown point is X ≈ 525 mm (X/c ≈ 0.55). These results do not show any change in the vortex flow structure when control is activated. Injection moves the breakdown location downstream (by about 50 mm). Figure 7 gives a comparison of the axial and normal velocity component profiles at a distance ΔX upstream and downstream of breakdown. For this type of comparison, it is necessary to take modifications of the external pressure gradient into account, as this can influence the flow. The profiles show good agreement between the two configurations for both the axial and tangential velocity components.

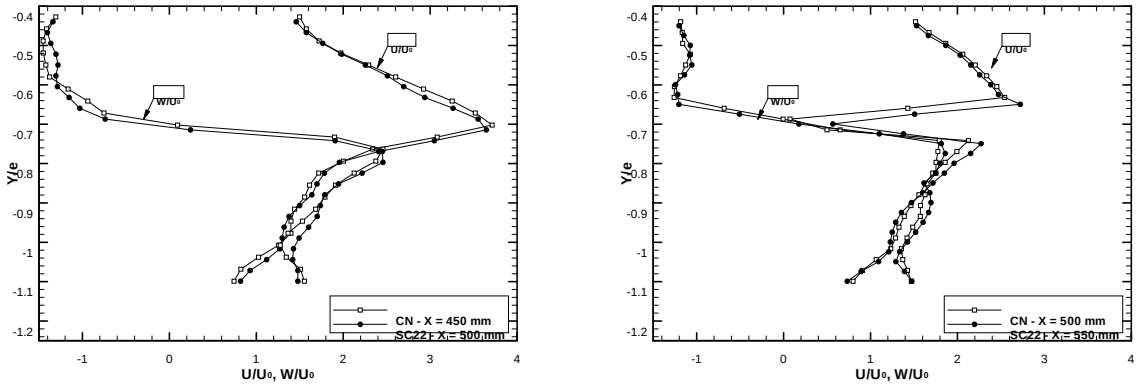

a – Upstream of breakdown

b – Downstream of breakdown

Fig. 7 – Comparison of the velocity profiles upstream (a) and downstream (b) of breakdown with control (SC22) and without control (CN).

Continuous injection amounts to adding momentum to the flow. Momentum is added not only to the core of the vortex but is also distributed throughout the rotating system and has the effect of moving the phenomena downstream. The vortex structure is shifted downstream but its structure is not modified.

A correlation between the vortex breakdown location and the instantaneous surface pressure distributions has been demonstrated. For an angle of attack α = 30 degrees, breakdown is located at X = 475 mm for the nominal configuration. When continuous injection is activated, the breakdown point moves downstream to X = 525 mm. Figure 8 compares the power spectral density distributions obtained for the normal configuration and for the configuration with injection at Q_m = 2.2 g/s (C_μ = 0.006).

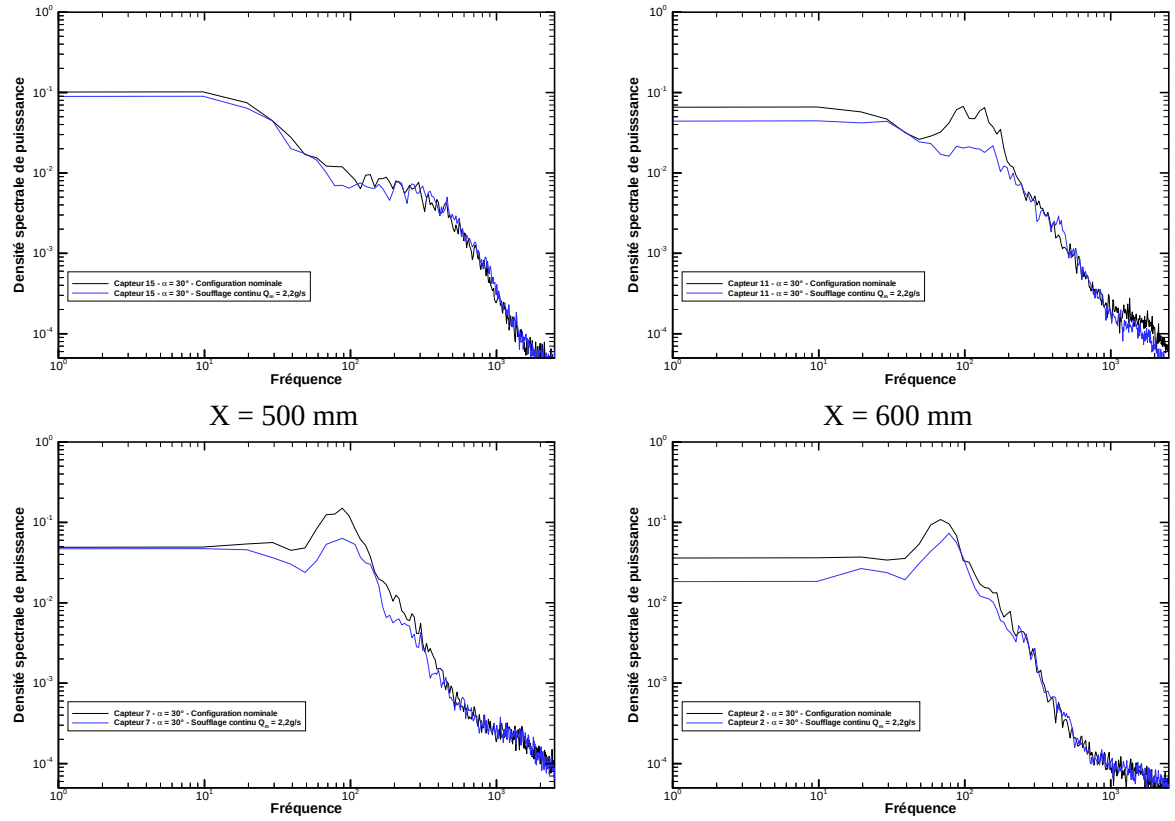

X = 500 mm X = 600 mm

X = 700 mm X = 800 mm

Fig. 8 – Influence of control by injection on the power spectral density.

A substantial attenuation of the power spectral density in the 40-120 Hz range can be observed at X = 600 mm for the configuration with injection. A slight decrease in the power spectral density extremum is observed for the following stations (X = 700 and X = 800 mm). From the standpoint of the instantaneous surface pressure variations, injection has an effect similar to a decrease in the model's angle of attack.

Effect of control by pulsed injection. For this part of the study, the effects of injection were analyzed at X = 600 mm. Figure 9 shows the power spectral density distributions for all the configurations investigated. The results obtained for continuous injection are consistent with the observations made above. For the case corresponding to an injection rate Q_m = 1.8 g/s (C_μ = 0.005), a decrease in level and a frequency shift of the power spectral density peak are observed. The results obtained for injection rates of 2.2 g/s and 3.2 g/s do not exhibit any differences for this study. In both cases, the vortex breakdown location moves downstream and can no longer be detected at X = 600 mm from the surface pressures.

Pulsed injection was studied at an injection rate Q_m = 3.2 g/s (C_μ = 0.009) for three different frequencies: 0.5, 1 and 10 Hz. Differences in behavior were observed for each of the three frequencies. For instance, at f = 10 Hz, the spectral density distribution was similar to that obtained for the continuous injection configurations. This gives reason to believe that the effects on the location of

vortex breakdown are of the same order. Frequencies f = 0.5 and f = 1 Hz lead to effects between those obtained for the nominal configuration and those obtained for continuous injection and pulsed injection at 10 Hz. The tests conducted with pulsed injection were an initial approach to this type of control. The results demonstrated that the frequency of pulsed blowing has an effect on the efficiency of control.

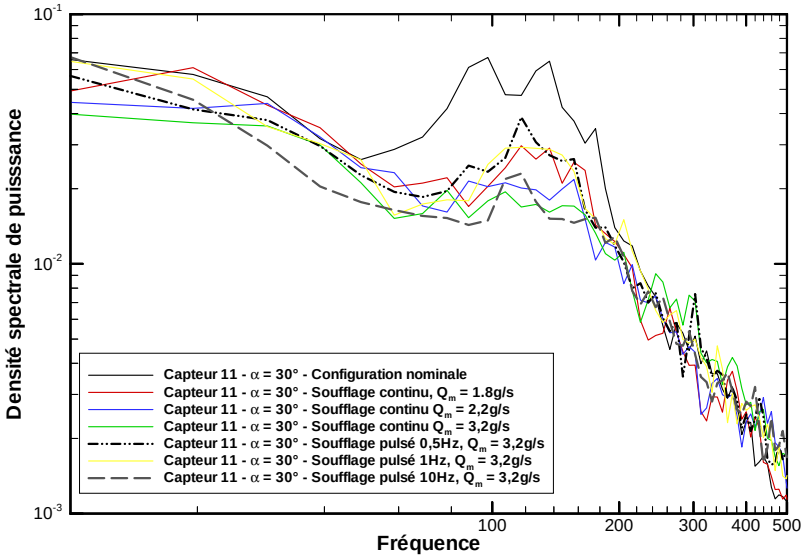

Fig. 9 – Influence of control by continuous and pulsed injection on the power spectral density.

3 Water Tunnel Investigation of Vortex Breakdown Control

3.1 Experimental Set-up

The tests were conducted in a vertical water tunnel whose test section has a cross section of 300×300 mm^2 and a length of 1 m. The sidewalls can be equipped with 280×400 mm^2 windows to observe the flow over the complete length of the test section and in both directions normal to the freestream velocity. The flow velocity is continuously controlled by two separate pumps and can vary from 0 to 1 m/s.

The test model was a delta wing with a 60-degree sweep and a chord c = 86.6mm. The relative wing thickness was $e_p/c = 0.087$. The leading edges were beveled at 50 degrees and tapered. Two geometrically identical models were made. One had eight heated wires located along the edges. These heating elements were in contact with as many separate metal plates flush with the bevel and were used to dissipate the heat energy in the vicinity of the separation lines. This system produces local thermal markings of the turbulent structures in the flowfiel so they can be viewed by schlieren imaging [12]. A second model, geometrically similar to the first, was equipped with an internal three-component balance (lift, roll and pitch). The upper surfaces of the models were equipped with eight swiveling nozzles in a plane parallel to the wing. The orifices had a diameter d of 0.8 mm in the injection plane. The tests were conducted for two different injection directions: the freestream direction corresponding to an azimuth angle θ = 180 degrees, and parallel to the leading edges corresponding to θ = 150° (see Fig. 10).

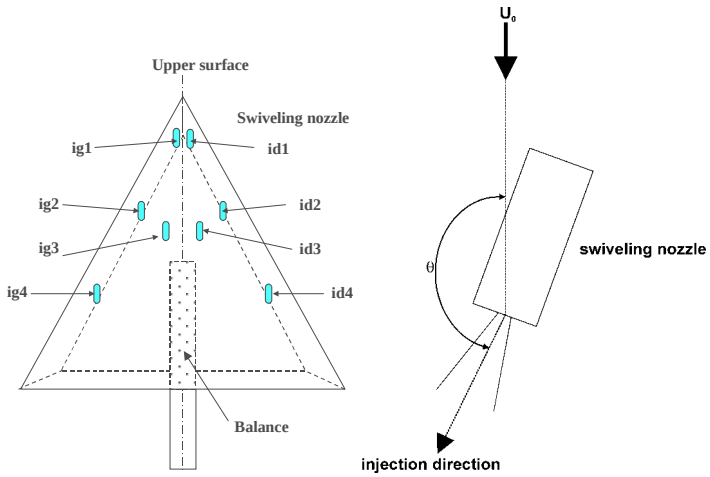

Fig. 10 - Diagrams of the model and an injector

A balance included in the model measured the normal force Fn as well as the pitch and roll moments My and Mx. It had a sensitivity of 5% of the measured forces for U_0 = 0.1m/s and of 0.5% for U_0 = 1m/s. The distance from the apex to the center of reference of the balance was equal to 2c/3. The visualization methods used included schlieren imaging with local thermal marking of the turbulent structure and the usual technique of colored streaks emitted at very low velocities from the injectors and coupled with a laser sheet. Schlieren imaging gives an overall view of the vorticity field. Used in conjunction with dye emission, it also gives the shadow of the emission line in the complete vorticity field. In the presence of vortex breakdown, these techniques allow tracking of the vortex breakdown location and observation of the behavior of the dye in the vortex environment. Since schlieren imaging is integrative, it gives an image of a strong 3-D phenomenon integrated along the span, which complicates analysis of the images and in particular, that of the paths. This drawback is partly overcome by the information supplied by the laser sheet visualization.

3.2 Test Procedure

The tests were conducted with injection for angles of attack α = 20, 30, 40, and 50 degrees and for freestream velocities U_0 = 0.10 m/s and 0.15 m/s, corresponding to chord based Reynolds numbers Re = 8,660 and 13,000 respectively. The goal of this experiment was to demonstrate the ability of the flow injection to modify the vortical flowfield and the vortex breakdown location.. In this initial approach, the Reynolds numbers were relatively low and the values of the injection momentum coefficient C_μ, defined above, were relatively high. This choice was dictated for the following reasons:

- Video recordings of the visualizations require a relative low freestream velocity to keep the sampling rate consistent with the time scales characteristic of unsteady phenomena
- The sharp leading edges are extremely stable separation lines. It is therefore necessary to use relatively high energy jets, corresponding to high values of C_μ, to move the vortex breakdown locations downstream. This was achieved only for relatively low values of the Reynolds number.

3.3 Presentation of the Results

Figure 11 shows the modifications induced in the flow by injection through injector ig2 parallel to the leading edge. Without injection, it is observed that the separation lines give rise to the emission of roughly parallel vortex structures (see Fig.11a). With injection, the flow appears to reattach to the upper surface (see Fig.11b).

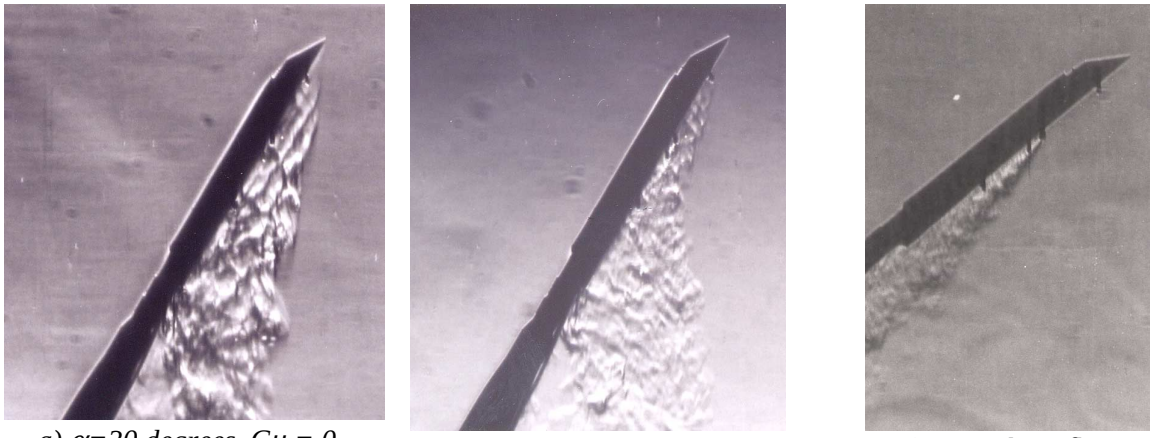

a) α=30 degrees, Cμ = 0., Re=8,660

b) α=30 degrees, Cμ= 0.02, Re=8,660

c) Jet without flow

Fig. 11 - Schlieren images of the flow

Figure 11c shows the jet structure in the absence of a flow. Comparison of this image with Figure 11b demonstrates the existence of a very strong interaction between the jet and the vortex. The jet modifies the vortex structure, whose breakdown location moves downstream. In return, the vortex pulls the jet in a direction different from its initial direction, and which seems imposed by the structure resulting from the vortex (see Fig. 12).

a) by ig4

b) by ig2

Fig. 12 – Injection parallel to the chord – $\alpha=20^{O}$, Cμ=0.02, Re=8660.

From this point of view, the injection direction appears to be a relatively insensitive parameter provided the initial separation between the vortex axis and jet axis is small enough for coupling to occur. In all cases, a lateral movement of the vortex core toward the wing tip accompanies the downstream movement of the vortex breakdown. The point of intersection between the vortex core and the jet axis determines the farthest downstream location of vortex breakdown. The existence of this point shows why delaying the breakdown phenomena by fluid injection is asymptotic. Additionally, for a given total injection rate, it appears unnecessary to use several injectors, since the downstream movement of vortex breakdown is limited by the intersection of the vortex with one of the jets, therefore canceling the contribution of the other jets.

For a given jet direction, strong interaction with the vortex is facilitated if the vortex is large, *i.e.* at the highest angles of attack. On the contrary, at the lowest angle of attack, 20 degrees, the accuracy of the injection direction is significantly more important. However, the larger the vortex, the earlier it needs to be controlled, for a constant injection rate, in order to move the breakdown location downstream. But since downstream movement is limited by the intersection between the jet and vortex, the injection point must not be located too far upstream, or it will prevent downstream movement of the breakdown location. For a given angle of attack, there is probably an optimal chordwise position of the injection point.

Since strong interaction causes the vortex to move toward the wing tip, it can be understood why injections parallel to the leading edge are always more efficient. The directions of the two structures are then more or less aligned. However, it could be expected that moving the injection point on the span towards the wing axis could move the vortex breakdown location further downstream, provided the jet direction was suitably adjusted. This would increase the angle between the jet and vortex, thereby moving the point of intersection between the two structures downstream. This idea is supported by the observation that injection by id3 or ig3 parallel to the leading edge is always very efficient. However, it does not appear very consistent with the fact that the controlled vortex more or less imposes its structure on the jet, which means that the jet direction may be a relatively minor parameter. This point remains to be investigated as it would allow determination of an optimal jet direction and spanwise location for a given injection rate.

Asymmetric injection generates a large roll moment, of the same order as that caused by deflection of a flap. This implies that it would be possible to use the jet as a lateral control system at high angles of attack (see Fig.13). Whatever the angle of attack, the gains on the normal force are between 15 and 25 percent for Cμ = 0.02 constant.

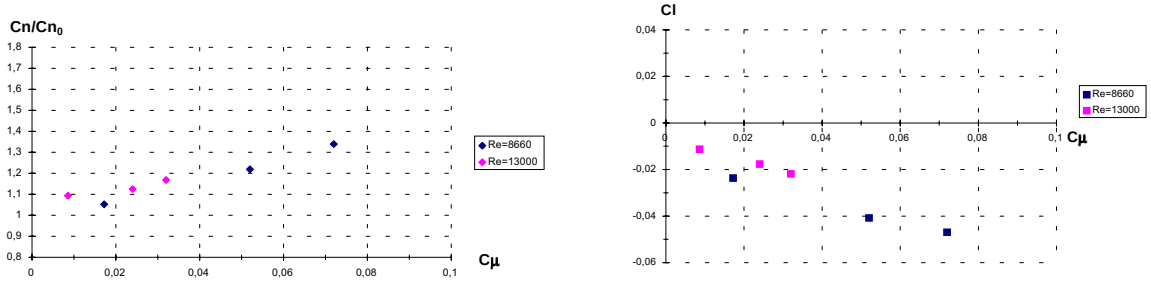

Fig. 13 - Effect of injection parallel to the chord on roll and lift - α=40 degrees

4 Conclusion

Two experiments investigating control of vortex breakdown on a delta wing by fluid injection are described. The first study was conducted in a wind tunnel on a wing with a 70-degree sweep and focused on characterizing breakdown by analyzing the unsteady pressures on the leeward surface of the wing. A peak in the power spectral density of the unsteady pressure signal occurred a certain distance downstream of the mean vortex breakdown location. The frequency of this peak decreased as the distance from the sensors to the vortex breakdown location increased, in correlation with amplification of the fluctuations arising at vortex breakdown. However, there were too few pressure sensors in this experiment to allow accurate determination of the fluctuating breakdown location. It was also shown that along-the-core fluid injection near the apex causes the breakdown location to move downstream. This manipulation of the phenomenon was detected by both field measurements and by unsteady pressure sensors on the suction surface of the delta wing. This study represents the first step towards the ultimate goal of observing the vortex breakdown phenomenon using unsteady surface pressure measurements to provide a feedback signal for closed-loop automatic control. Work is continuing on a wing equipped with more unsteady pressure sensors.

During the second experiment, the results obtained in the water tunnel on a wing with a 60-degree sweep for injection in several locations on the wing demonstrated the efficiency of momentum injection for controlling the vortex breakdown location. These results were, however, obtained with a simplified model and under relatively severe flow conditions. Work will be continued with pulsed injection on a more representative model equipped with rounded leading edges. Injection will then be possible at higher Reynolds numbers. Since the applied loads will be stronger, the measurement accuracy will also improve.

5 References

[1] Roy, M. *Caractères de l'écoulement autour d'une aile en flèche accentuée*. C.R. Acad. Sc. 234, pp. 2501-2503, 1952

[2] Legendre, R. *Ecoulement au voisinage de la pointe avant d'une aile à forte flèche aux incidences moyennes*. La Recherche Aéronautique, N° 30, pp. 3-8, 1952

[3] Hummel, D.*On the vortex formation on a delta wing at large angle of incidence*. AGARD CP 247, 1978

[4] Payne, F.M., Ng, T.T., Nelson, R.C. and Schiff, L.B. *Visualization and flow surveys of the leading edge vortex structure on a delta wing planform*. AIAA Paper 86-330, 1986.

[5] Kegelman, J. and Roos, F. *Effects of leading-edge shape and vortex burst on the flowfield of a 70 degree sweep delta-wing.* AIAA Paper 89-0086, 1989

[6] Ng, T.T. and Oliver, D.R. *Leading edge vortex and shear layer instabilities*. AIAA Paper 98-0313, 1998

[7] Werlé, H. *Etude phénoménologique de la formation et de l'éclatement des tourbillons au tunnel hydrodynamique TH2*. Onera, RT 29/1147 AY, septembre 1985

[8] Délery, J. *Aspects of vortex breakdown*. Prog. Aerospace Sci., Vol. 30, pp. 1-59, 1994

[9] Pagan, D. et Solignac, J.L. *Etude expérimentale de l'éclatement d'un tourbillon engendré par une aile delta* La Recherche Aérospatiale, N°. 3, pp. 197-219, mai-juin 1986

[10] Molton, P. *Etude expérimentale de l'éclatement tourbillonnaire sur aile delta en écoulement incompressible. Caractérisation du champ externe*. Onera, RT 53/1147 AN, juin 1992

[11] Mitchell, A. *Caractérisation et contrôle de l'éclatement tourbillonnaire sur une aile delta aux hautes incidences*. Thèse de doctorat de l'Université Paris 6, 07-2000

[12] Rodriguez, O. *Base drag reduction by control of the three-dimensional unsteady vortical structures.* Exp. In Fluids 11, pp.218-226, 1991

Paper: 19
Author: Mr. Molton

Question by Dr. Luckring: First let me comment that it is very good to show the repeat measurements and the scatter in data for vortex breakdown location. Question: Are there Reynolds number effects or sensitivities for your results?

Answer: Tests were done for chord Reynolds numbers (Re_c) from 650,000 to 2,600,000 and we did not observe any influence of Reynolds number on the location of vortex breakdown. Reynolds number changes did influence the secondary vortices and the location of transition from laminar to turbulent flow. The vortex breakdown locations measured here also compare well to water tunnel tests at much lower Re_c. The insensitivity to Re_c is primarily due to the sharp leading edges of the delta wings tested.

This page has been deliberately left blank

Page intentionnellement blanche